



# An Improved Coupled Hydrologic-Hydrodynamic Model for Urban Flood Simulations Under Varied Scenarios

Siwei Cheng<sup>1,2,3</sup> · Mingxiang Yang<sup>3,4</sup>  · Chenglin Li<sup>1,2</sup> · Houlei Xu<sup>5</sup> · Changli Chen<sup>5</sup> · Dewei Shu<sup>5</sup> · Yunzhong Jiang<sup>3,4</sup> · Yunpeng Gui<sup>3,4</sup> · Ningpeng Dong<sup>3,4</sup>

Received: 24 April 2024 / Accepted: 7 June 2024  
© The Author(s), under exclusive licence to Springer Nature B.V. 2024

## Abstract

Cities place a high priority on addressing urban flooding issues and have worked on flood prevention planning and construction efforts. This study aims to develop the improved coupling hydrologic-hydrodynamic model based on SWMM and TELEMAC-2D model by considering river runoff factors. Taking Tongzhou district of Beijing as an example, two different coupled models of the drainage network are constructed for comparison. The research focused on the drainage capacity of the study area and surface ponding water under different rainfall recurrence periods to evaluate the current flood resilience status and the priority of drainage network improvements. The results indicate that the demonstration area effectively mitigates urban flooding and can handle a 100-year return period rainfall event, with a maximum inundation depth of 0.407 m and an overflow node ratio of 20.8%. As the rainfall recurrence period increases, the number of overflow nodes tends to stabilize. Due to the high susceptibility of traffic hubs in cities to flooding, the result of contrast model analysis suggests prioritizing the drainage networks under main roads and overpasses and implementing Low Impact Development (LID) facilities around rivers to enhance urban infiltration and reduce river overflow risks. This coupled model demonstrates good applicability and high simulation accuracy for complex urban flood scenarios, emphasizing the importance of targeted urban planning and infrastructure improvements in enhancing flood resilience.

**Keywords** Coupled model · Urban flood · Urban hydrology · Drainage network · Beijing

## 1 Introduction

Amid global warming and rapid urbanization, changes in urban rainfall and runoff patterns, a continual decline in soil infiltration capacity, and the lagging development of drainage infrastructure have increased the risk of urban flooding, resulting in significant economic losses (Zhao et al. 2023). China is also one of the regions where heavy rainfall and flooding occur frequently with 70% of its cities having suffered severe flood disasters, including 33% of its megacities (Chikhi et al. 2024). Urban flooding is primarily caused by overflow from the drainage network due to extreme rainfall and from rivers at high water levels (Ahmad and

---

Extended author information available on the last page of the article

Simonovic 2013; Yao et al. 2023). Thus, it is crucial to consider the affect river runoff in urban flood simulation models.

Numerical simulation plays a crucial role in exploring the internal dynamics and developmental processes of urban flooding (XU Zongxue and Chenlei 2021). Among the various numerical simulation tools, the Urban Stormwater Management Model (SWMM) is the most widely used. However, since this model cannot provide important information such as the extent of inundation, depth of flooding, and water flow velocity (Liu et al. 2023; Zhuang et al. 2023), researchers have coupled the SWMM with other two-dimensional modeling software to compensate for this shortcoming like LISFLOOD-FP, WCA2D and CCHE2D (Wu et al. 2018, 2017; Zeng et al. 2022; Zhang et al. 2021), and evaluate the city's flood defense capabilities and flood risk under different scenarios. The city is not a simple and flat catchment area, the underlying surface inside the city is complex, with irregularly shaped and arranged buildings, and numerous channels and rivers (Ouyang et al. 2022). The use of uniform grid sizes for simulating complex urban terrain often yields poor results. Theoretically, using irregular grids to solve the full or simplified two-dimensional shallow water equations for two-dimensional simulation can achieve more accurate inundation results.

The TELEMAC-2D model features stable two-dimensional hydrodynamic computation capabilities and is also suitable for further development. It is widely used to simulate hydrodynamic processes in rivers, estuaries, coastal areas, and floodplains, consistently providing dependable results (Kumar et al. 2021). Currently, the use of TELEMAC-2D in flood modeling is also becoming increasingly widespread, (Yang et al. 2023) developed a SWTM model to assess the flood impacts around Beijing's Fangzhuang subway station; (Chen et al. 2017) used coupled models to analysis flood inundation scenarios for coastal nuclear power plants under storm surge conditions. Similarly, (Guoyi and Jiahong 2022) established TELEMAC-2D model to assess flood risks in Shenzhen city and discussed inundation situation under different designed rainfall; (Rui et al. 2022) analyzed urban emergency response times under different flood scenarios with TELEMAC-2D model. However, the above studies have not considered the issue of river overflow under extreme rainfall conditions. The process of urban flood simulation is essentially a hydrological or hydrodynamic model, if without the factor of river runoff, the simulation accuracy of whole model will be affected.

This study proposes an improved model that considers the impact of river runoff within cities under extreme rainfall conditions based on hydrodynamic coupling of one-dimensional pipe network with SWMM model and TELEMAC-2D model. Taking the Tongzhou District of Beijing as example, a coupled urban flood model was constructed, and its reliability verified with over-standard design rainfall conditions and river levels as the initial conditions. In addition, we build a comparative coupled model by reducing the pipelines and nodes, distribution of flooding and surface inundation were uses as indicators to assess the urban flood risk under two different pipe network conditions. This works provides foundational support for the priority of subsequent sponge city theoretical transformations in various cities.

## 2 Methods

In this work, simulation was performed by hydrological-hydrodynamic model, where SWMM model and TELEMAC-2D model are used independently to simulate the processes of pipeline networks, surface and river runoff. Additionally, this model is unidirectionally coupled to facilitate flow exchange in three dimensions including vertical, lateral and longitudinal to ensure accuracy of the urban flood simulation.

## 2.1 SWMM Model

The SWMM (Storm Water Management Model) is a distributed hydrological and hydrodynamic modeling tool developed by the U.S. Environmental Protection Agency (EPA). It is widely utilized for urban flood management (Tan et al. 2024). However, the calibration of the SWMM model remains a key challenge. The fundamental working principle of SWMM model involves using the Horton formula for runoff production and confluence calculations (Gironas et al. 2010), while the computation of pipeline flows is calculated using the dynamic wave method (Hashemi and Mahjouri 2022; Li et al. 2022b), which is based on solving the one-dimensional Saint–Venant equations (Voevodin and Nikiforovskaya 2011).

Runoff calculation:

$$R_s = \int_{i>f_p} (i - f_p)dt \tag{1}$$

$$f_p = f_c + (f_0 - f_c)e^{-kt} \tag{2}$$

where,  $R_s$  is the surface runoff in mm;  $i$  is rainfall intensity in mm/h;  $f_p$  is infiltration capacity in mm/h;  $f_0$  is the infiltration capacity corresponding to the initial soil water content in mm/h;  $f_c$  is the stable infiltration rate;  $k$  is the decay coefficient;  $t$  is the time in h.

Pipe confluence calculation:

$$\frac{\partial Q}{\partial x} + \frac{\partial A}{\partial t} = q \tag{3}$$

$$\frac{\partial Q}{\partial x} + \frac{\partial}{\partial x} \left( \frac{Q^2}{A} \right) + gA \frac{\partial h}{\partial x} + gAS_f = 0 \tag{4}$$

Where  $Q$  is the discharge in  $m^3/s$ ,  $A$  is the area of the cross section in  $m^2$ ,  $H$  is water depth in m,  $g$  is the acceleration of gravity in  $m/s^2$ ,  $S_f$  is the friction gradient, which is calculated by manning formula.

## 2.2 TELEMAC-2D Model

TELEMAC-MASCARET is an open-source hydraulic modeling system for rivers, estuaries, and coasts, featuring one-dimensional, two-dimensional, and three-dimensional models, developed by the National Laboratory of Hydraulics and Environment in France (Moulinec et al. 2011), it is primarily managed by a consortium of consulting and research institutions. TELEMAC-2D used in this paper is one of the two-dimensional hydrodynamic calculation modules. This module is primarily used for solving two-dimensional shallow water equations, calculating water depths and flow velocities at each node. It is widely applied in extensive storm surge and flood simulations along coasts, although its specific application for urban flood inundation simulations is relatively less common (Godara et al. 2023). In this study, the finite volume method in TELEMAC-2D is adopted to solve the two-dimensional shallow water dynamic equation in non-conservation form (Malcherek 2000). The basic equation is as follows:

$$\frac{\partial h}{\partial t} + \frac{\partial(hu)}{\partial x} + \frac{\partial(hv)}{\partial y} = 0 \quad (5)$$

$$\frac{\partial u}{\partial t} + u \frac{\partial u}{\partial x} + v \frac{\partial u}{\partial y} = -g \frac{\partial Z}{\partial x} + F_x + \frac{1}{h} \text{div}(hv_e \nabla u) \quad (6)$$

$$\frac{\partial v}{\partial t} + u \frac{\partial v}{\partial x} + v \frac{\partial v}{\partial y} = -g \frac{\partial Z}{\partial y} + F_y + \frac{1}{h} \text{div}(hv_e \nabla v) \quad (7)$$

Where,  $u$  and  $v$  are depth integrated velocity components in the  $x$  and  $y$  directions, respectively;  $h$  is flow depth;  $Z$  is water surface elevation;  $t$  is time;  $g$  is gravity;  $v_e$  is the effective diffusion for turbulent viscosity and dispersion; and  $F_x$  and  $F_y$  are source terms that ignore the Coriolis force and the influence of wind.

$$F_x = -\frac{1}{\cos \alpha} \frac{gm^2}{h^{4/3}} u \sqrt{u^2 + v^2} \quad (8)$$

$$F_y = -\frac{1}{\cos \alpha} \frac{gm^2}{h^{4/3}} v \sqrt{u^2 + v^2} \quad (9)$$

Where,  $\alpha$  is bottom slope dip angle. Equations (5)-(7) are solved for three unknowns  $h$ ,  $u$ , and  $v$ , and the boundary conditions and meshes are set by the user in the BlueKenue software (<https://nrc.canda.ca/en>). In this study, TELEMAC-2D version of V8P4 was used for simulation, and unstructured grid was used to segment the grid region.

### 2.3 1D-2D Coupled Model

In this research, we have incorporated the calculation of river runoff into our coupled SWMM and TELEMAC-2D model. The steps are as follows:

Step1: Basic data processing. The data of the study area is generalized based on ArcGIS pro platform, including the information of inspection wells, pipeline networks, outfalls, rain measuring station and river monitoring station.

Step2: Pipeline correction and sub-catchment area division. The reality pipe network data must have problems such as crossing, reverse slopes, leaks and incorrect connections. Therefore, we adjusted incorrect pipes by removing unnecessary short pipelines and appropriately modifying the elevations of the nodes on both sides of the pipelines with reverse slope. The check rules with the following verification rules: (1) The direction of pipelines must flow from the upstream node to the downstream node. (2) The bottom elevation of the upstream node must higher than that of the downstream node. (3) The flow direction of water in any node or pipe within the area must flow into only one outlet. Sub-catchment areas were manually divided based on these corrections and actual road network.

Step3: Parameter calibration and verification. Parameter calibration in the SWMM model is a crucial step that determines the overall accuracy of the simulation. Using the pyswmm library combined with the genetic algorithm (GA), sensitive parameters are calibrated by

directly reading simulated depths at monitoring nodes or flow velocities in pipes. When the fitness > 0.9, the calculation is terminated, and the parameter values are obtained.

Step4: Point source parameter file. The overflow point time series and the position of the inspection well nodes were extracted and written into the parameter file of TELEMAC-2D.

Step5: River level's file. During river simulation, it is necessary to set water levels to ensure river flow continuity. In the process of extreme rainfall, simulations are conducted using water levels that exceed standard levels as specified in planning, and these levels' data are then written into the parameter files.

Step6-7: Geometry file and boundary file. In this study, BlueKenue software was used to pre-process geometry files and boundary files in TELEMAC-2D. The geometry files, which includes elevation data and surface manning coefficients, are assigned to the mesh file using 2D interpolators. The setup of boundary file designates the upstream of the river as the mesh entrance, where the water level or flow velocity is specified, and the downstream of the river is set as the exit boundary of the mesh.

Step8: Analyze the urban flood simulation based on inundation position、depth、area and duration.

The methodology and process of this research are illustrated in Fig. 1.

### 2.4 Model Evaluation Indicator Selection

The absolute error represents total value of the difference between the measured value and the actual value. Here, it refers to the total value of the difference between the simulated water depth or outfall volume of the model and the actual measured water depth/outfall volume (Hu et al. 2018). The mathematical expression is as follows:

$$AE = |T_s - T_o| \tag{10}$$

where,  $T_s$  and  $T_o$  are the simulated and observed flow rate at the  $i$  th number.

The relative error is calculated by multiplying the ratio of the absolute error from the measurement by the actual measured value by 100% and is expressed as a percentage. Typically, relatively error provides a more reliable indicator of measurement accuracy. It is commonly used to assess urban rainfall and flood models, particularly to verify the accuracy of simulated peak flood discharge values (Indrawati et al. 2018). It is described as follows:

$$RE = \frac{|R_s - R_o|}{R_o} \times 100\% \tag{11}$$

where,  $R_s$  and  $R_o$  are the simulated and observed flow rate at the  $i$  th number.

The Nash–Sutcliffe Efficiency mathematical expression of this matric can be described as follows:

$$NSE = 1 - \frac{\sum_{i=1}^n (Q_s - Q_o)^2}{\sum_{i=1}^n (Q_s - \bar{Q}_o)^2} \tag{12}$$

where,  $Q_o$  ( $m^3/s$ ) and  $Q_s$  ( $m^3/s$ ) represent the discharge of the observed and simulated hydrography, respectively;  $\bar{Q}_o$  is the mean value of the observed discharge, and  $n$  is the data points number.  $NSE$  measures the ability of the model to predict variables different from the mean, gives the proportion of the initial variance accounted for by the model,

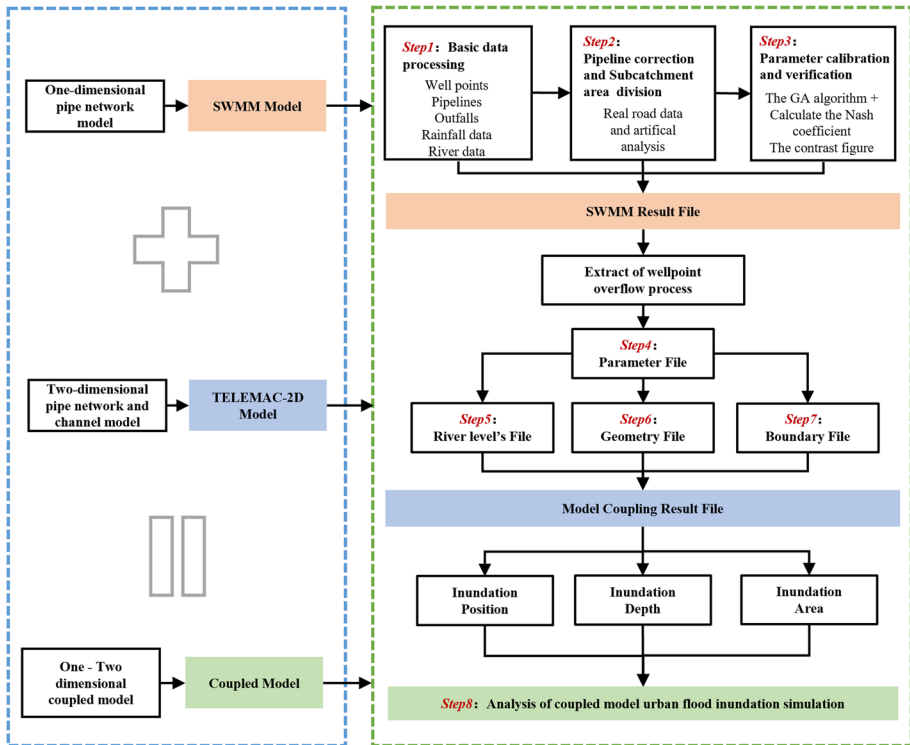


Fig. 1 Flowchart of urban flood simulation coupled model

and ranges from 1 (perfect fit) to  $-\infty$ . Values closer to 1 provide more accurate predictions (Nash and Sutcliffe 1970).

### 3 Study Area and Materials

#### 3.1 Study Site

In this study, we have selected the sponge city planning pilot area of Beijing's Tongzhou district urban sub-center which covered a total area of 19.36 km<sup>2</sup> and encircled by the Yunchaojian River and the North Canal. The average slope of study area is approximately 1.38%, the annual average rainfall surpasses 500 mm, with about 85% of it concentrated between June and September. The implementation of sponge city infrastructure transformations has been successfully completed in this study area, establishing flood prevention standards of 50-year return period for general areas and 100-year return period for the administrative office zone (Yajun et al. 2021).

### 3.2 One-Dimensional Pipeline Network Model Build Processing

#### 3.2.1 Data Preparation

Topographic inputs are crucial in the process of constructing urban rainstorm and flood model, which includes digital elevation data and land use data. We utilize the STRM 12.5×12.5 m digital elevation model (DEM) is drawn from the NASA (<https://search.earthdata.nasa/>). Remote sensing data is from Globeland 30 (<http://www.globallandcover.com/>), which provides “Gaofen-1” satellite imagery with a spatial resolution of 16 m. These data all correspond to the surface characteristics of the study area (Fig. 2).

Drainage system data were provided by the Tongzhou District Water Bureau of Beijing. These data primarily include the geographical and geometric information of pipelines, inspection wells, and outfalls. The diameters of the pipes within the drainage system range from 0.6 to 2.6 m, and the depths of inspection wells range from 0.5 to 6.4 m. The study area contains two rivers, the North Canal and the Yunchaojian river, which have been artificially modified and considered as rectangular open channels, as shown in Fig. 3. The original model comprises 78 sub-catchment areas, 632 pipelines, 619 inspection wells, and 12 outfalls. In the contrast model, we reduced the number of pipelines and nodes under main roads and interchanges, resulting in 496 pipelines, 491 inspection wells, and 9 outfalls, with specific differences shown in Fig. 3c-d.

Furthermore, we adopted the rainstorm intensity formula provided by the Beijing Water Bureau to calculate surface rainfall. The Chicago rainstorm model (Su et al. 2021) was selected as the design rain pattern for this research, with a peak rainfall coefficient set at

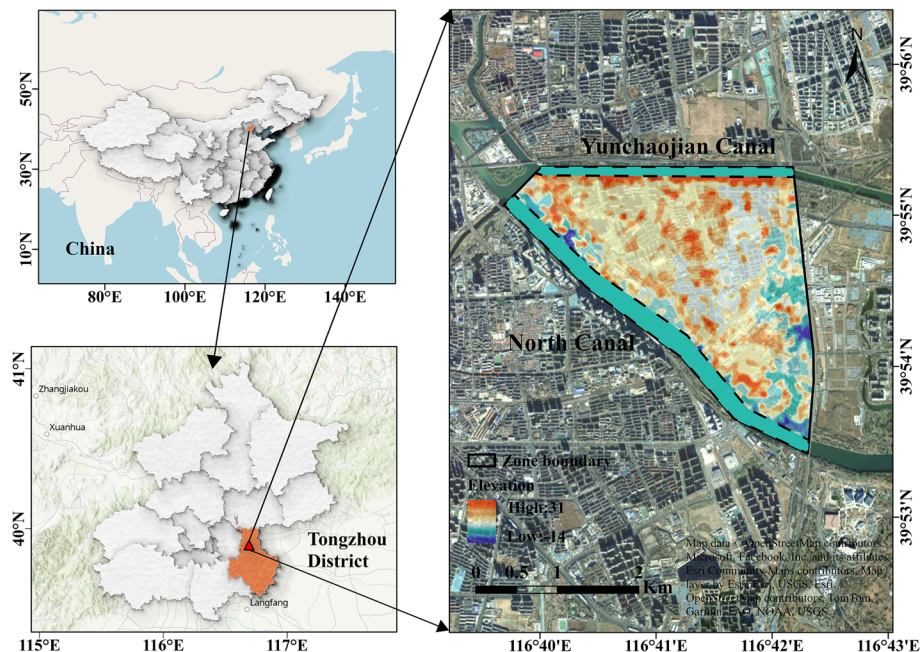
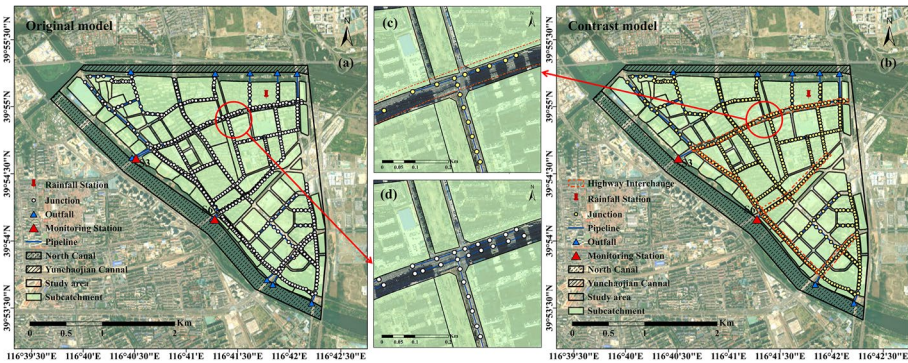


Fig. 2 Study area



**Fig. 3** The difference of pipeline distribution map with two models

0.4. This approach facilitated the computation of rainfall data for of 120 min across eight different return periods, serving as the input for our modeling efforts. The design rainstorm formula as followed:

$$q = \frac{1602(1 + 1.037 \lg P)}{(t + 11.593)^{0.681}} \quad (13)$$

where,  $q$  is the rainfall intensity mm/hr;  $P$  is the return period of rainstorm in yr;  $t$  is the rainstorm duration in min.

### 3.2.2 Parameters of SWMM Model

The deterministic parameters of SWMM model include characteristics such as the width of sub-catchments, average slope and the proportion of impervious areas (Li et al. 2017). The characteristic length of a sub-catchment is obtained by dividing its area by the perimeter of its drainage area. The average slope is calculated from digital elevation data. The proportion of impervious areas is calculated based on the hardened area divided by the total area within land use data.

In this research, sensitive parameters within uncertain parameters were calibration based on measured data (Liao et al. 2023), including the roughness coefficients for pervious and impervious areas, depression storage for pervious and impervious areas, the maximum and minimum infiltration formula, and Manning's coefficient in the pipeline. The range and results of parameter calibration are as follows (Table 1).

### 3.3 Two-Dimensional Pipeline Surface and River Model Build Processing

In this study, TELEMAC-2D version of V8P4 was used for simulation, and unstructured grid was used to segment the grid region. The DEM data generally omits specific elevation details of buildings and bottom elevation of rivers. To account for the water-blocking effect of buildings, the building outlines are utilized as internal soft boundaries to create meshless islands within the study area. When constructing the grid with these soft boundaries, BlueKenue automatically resamples the building outline to maintain the continuity of the construction grid. The maximum side length throughout the research area is 20 m, with



**Table 1** Main parameter calibration results of SWMM

Parameter model	Parameter name	Units	Parameter scale	Value
Subcatchment	N-Imperv		(0.11, 0.05)	0.043
	N-perv		(0.05, 0.8)	0.49
	Dstore-Imperv	mm	(0.05, 20)	5
	Dstore-Prev	mm	(0.05, 20)	10
Horton Infiltration	Max-Rate	mm/h	(20, 240)	200
	Min-Rate	mm/h	(10, 150)	122
	Decay	h-1	(0.5, 10)	1.19
	DryTime	d	(1, 10)	2.51
Pipeline	Manning-N		(0.008, 0.5)	0.014

refinements made in areas with dense construction. For accurate representation of the riverbed elevation, we reduced the existing river elevation data by 10 m, establish boundaries along the river's sides, and ensured they connect with the surface grid to maintain overall grid connectivity.

There are 279,501 nodes and 540,501 grids after processing surface grid. The obtained digital elevation information and Manning coefficients for different land use types are interpolated into the grid as the initial processing step for the simulation calculations. TELEMAC-2D river confluence simulation was adopted in this study, and the upper and lower reaches of the river were used as the boundary of the model. Due to the lack of measured flow change data of the river and the insignificant change of river level within 120 min in the measured data, the river level of is set at 20 m for the Yunchaojian River, and 18 m for the North Canal. The river levels have been set to exceed the planning standards for 20-year recurrence interval, to ensure the rationality of the water level difference and the flow of the river, and at the same time, the impact of the river overflow can be analyzed.

## 4 Results

### 4.1 Coupled Model Calibration and Evaluation

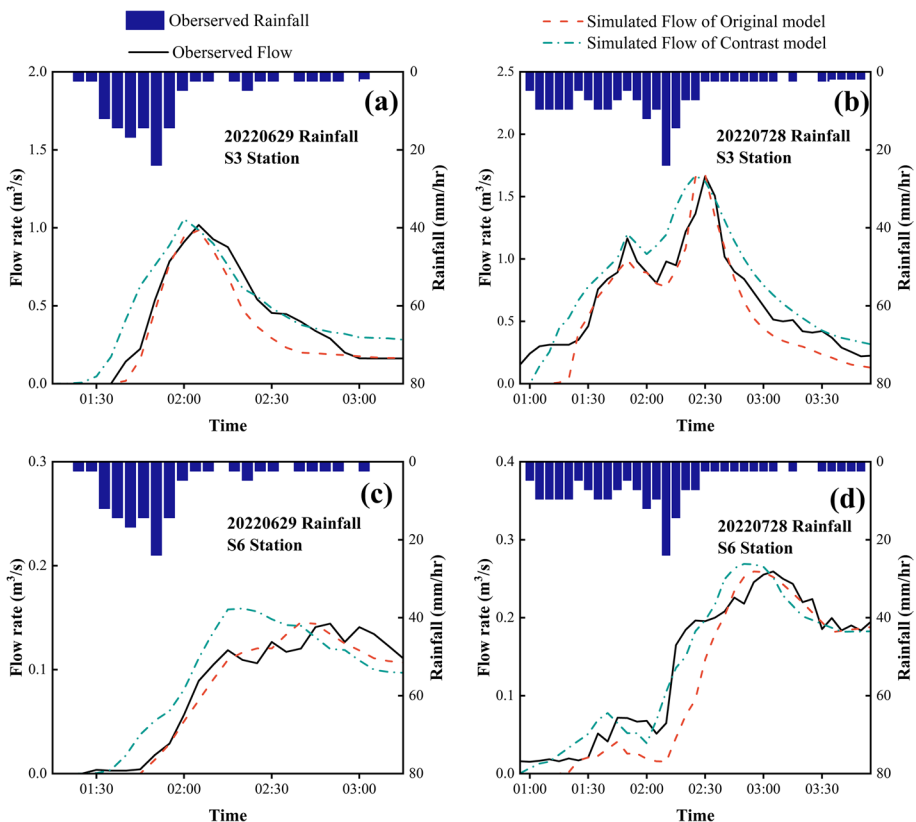
We selected No.20220629 and No.20220728 two historical measured rainfall data to calibrate and verify two coupled models, the results show in Table 2. Rainfall data mainly provided by Beijing Tongzhou District Water Bureau, is recorded every 5 min. Figure 4 shows that the simulated data of S3 and S6 monitoring points are closely align with the observed data, and the original model is higher accuracy with *NSE* value above 0.8. In the contrast model, where the number of pipelines and nodes was reduced, the *NSE* value remained above 0.7. The simulated flow rates increased, and the peak flow occurred 20 min earlier compared to the original model, with longer recession times.

### 4.2 Analysis of Inundation Result Under Eight Different Rainstorm Patterns

In the case of eight designed rainstorms, the original model and the contrast model were respectively carried out to reproduce rainfall, the location of flooding points and the depth of water were statistically analyzed. The results show that as the recurrence interval of rainfall increases, the volume of ware and inundation at internal flooding points

**Table 2** Calibration evaluation parameter

Storm	Monitoring Station	Nash coefficient		Relative Error		Absolute Error	
		Original	Contrast	Original	Contrast	Original	Contrast
20220629	S3	0.885	0.823	3.2%	3.7%	0	5
	S6	0.957	0.703	1.6%	9.11%	5	30
20220728	S3	0.821	0.761	2%	0.2%	0	5
	S6	0.812	0.935	0.3%	3.8%	10	20

**Fig. 4** Comparison of model calibration

gradually. The number of overflow points in both models approached similar counts, but in original model, the number of overflow points was closed to 20% of the total nodes, while in the contrast model it was closer to 28% (Table 3). Approximately 40% to 50% of the inundation points are distributed under the primary roads and overpasses with heavy traffic, and the undeveloped building land, while about 20% to 30% occur around

**Table 3** Comparison table of number of overflow points

Recurrence interval	Number of overflow points		Proportion	
	Original	Contrast	Original	Contrast
$P=1$	14	20	2.3%	4%
$P=3$	45	46	7.2%	9.4%
$P=5$	50	53	8.1%	10.7%
$P=10$	85	88	13.7%	17.9%
$P=20$	89	120	14.4%	24.4%
$P=30$	98	121	15.9%	24.6%
$P=50$	105	128	16.9%	26%
$P=100$	129	134	20.8%	27.2%

**Table 4** Changes in maximum inundation depth and area

Recurrence interval	Maximum inundation depth (m)		Inundation area (m <sup>2</sup> )	
	Original	Contrast	Original	Contrast
$P=1$	0.023	0.041	13261.67	23427.21
$P=3$	0.061	0.083	96842.81	113798.08
$P=5$	0.087	0.122	155941.74	189981.56
$P=10$	0.156	0.231	218946.32	280283.53
$P=20$	0.283	0.335	306948.66	386895.12
$P=30$	0.358	0.439	372685.36	478839.42
$P=50$	0.398	0.471	448837.39	575652.75
$P=100$	0.407	0.498	553803.19	666760.67

riverbanks in green belts. This high consistency with actual flood prone areas further substantiates the credibility of the model.

Table 4 indicated the poor drainage along main road causes the depth and area of inundation in the contrast model to far exceed those in the original model, with a significant difference in the inundation area for a 100-year rainstorm return period event (Fig. 5), greatly impacting nearby traffic and residents. However, the overall inundation depth of both models did not exceed 0.5 m, suggesting that this area complies with the planning standards for resisting a 100-year extreme rainfall event. This study utilized four monitoring points to analyze the simulation results of the two models (Fig. 6). In residential areas and parks adjacent to rivers, the water level rises slowly under lower recurrence intervals of rainfall, but increases rapidly as the recurrence interval grows. The depth of water on primary and secondary roads is more closely related to the recurrence interval of rainfall. In the contrast model, the peak of the overall inundation depth occurs 20 min earlier, and the duration of inundation is longer, which has a more serious impact on traffic.

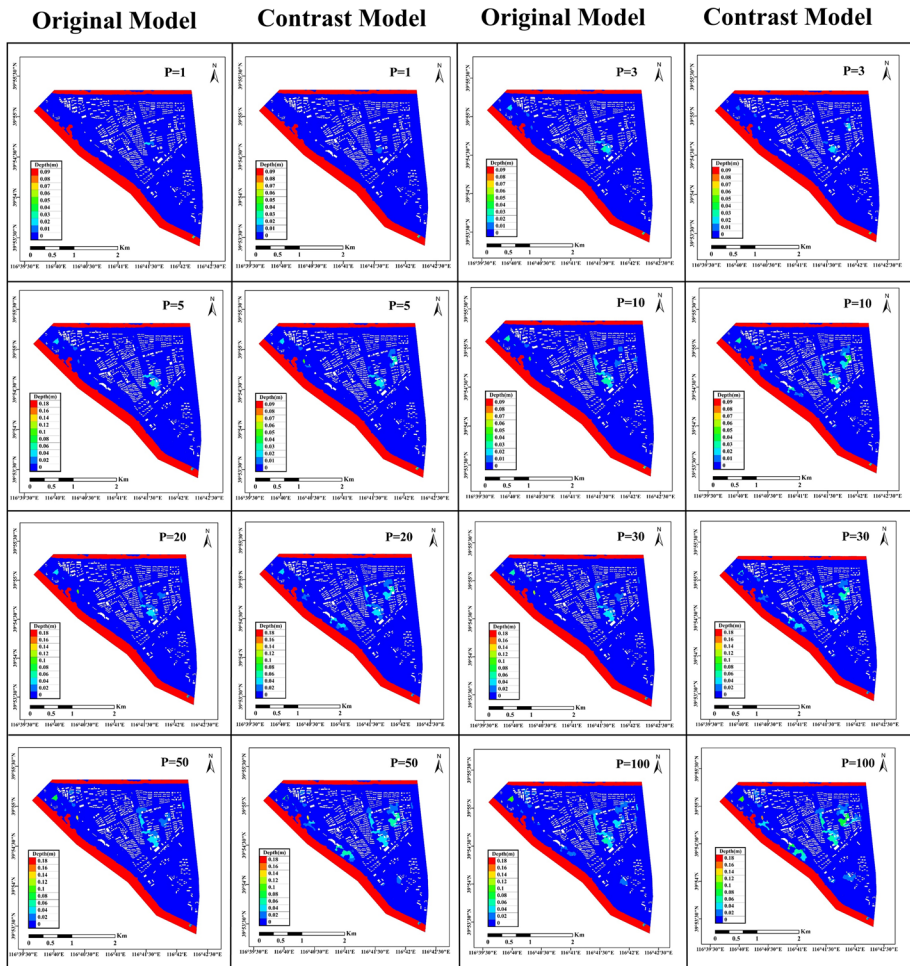


Fig. 5 Comparison of inundation between the two models

## 5 Discussion

It is well known that cities are not isolated from rivers. Many scholars choose to not to consider the influence of internal river flow when constructing urban flood simulation models due to the short duration of the simulation events (Liu et al. 2024; Ouyang et al. 2022; Xu et al. 2023; Yao et al. 2021). For this reason, (Chen et al. 2023) utilized the MIKE FLOOD model in Zhoukou City of Henan Province, setting an exceedingly high standard ware level as river's based level to analyze the impact of river levels on outlets. (Li et al. 2022a) treated the river as a huge drainage pipe in the urban flood simulation process in Luoyang City, analyzed the correlation between rainfall duration and inundation time. This research constructs the urban flood model is similar to above studies, regarding the river as a rectangular open channel with an ultrahigh standard river level as the basic condition for simulations. However, this study is distinctive in

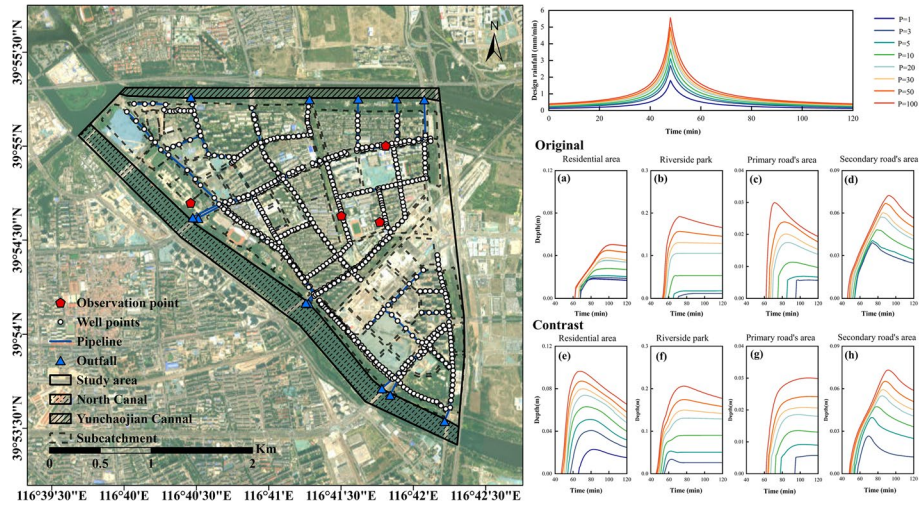


Fig. 6 Variation of inundation depth at observation point

that it exclusively uses open-source urban flooding, integrating post-processing tools to precisely analyze the internal water accumulation and the impact of river overflow.

Furthermore, in the result of the contrast model, it was found that in cities with high traffic volume, using just a single pipeline to generalize the number and location for overflow points does not cause significant changes. Therefore, it does alter the water collection situation in sub-catchment areas, and the flow rate, velocity, and the duration of inundation at overflow points increase greatly with the recurrence interval increases. This suggests that in situations where data is lacking, pipelines and nodes can be appropriately increased or decreased based on road levels and traffic volume to ensure the accuracy of the simulation.

Finally, this improved coupled hydrologic-hydrodynamic model based on SWMM and TELEMAC-2D, which considers the complexity of urban substrates and various factors affecting urban flooding, can be extended to urban areas with different terrain, including cities that have been transformed by sponge city projects. This provides insights for future large-city sponge city planning transformations. It is recommended to prioritize the renovation of pipelines under heavy traffic areas such as major roads and overpasses to reduce congestion in main pipelines, thereby preventing overflow and inundation in surrounding residential areas and effectively mitigating urban flooding to arrive planning objectives and flood protection standards.

### 6 Conclusion

This study has improved the coupled hydrologic-hydrodynamic model, considering an integrated urban flood coupled model that encompasses network overflow, surface runoff, and river flow. The main conclusions are as follows:

This model can simulate urban flooding with high precision. During the validation process, both the original and contrast models showed *NSE* value greater than 0.7, *AE* value less than 1 h, and *RE* value less than 10%. Additionally, within the study area, as the recurrence interval of rainfall increases, overflow points gradually shift towards

main roads, and both overflow volume and duration increase, leading to severe road inundation. This work based on open-source software, enhances the general applicability of the improved model and the diversity of post-processing methods. However, this paper still has limitations: the coupling model requires foundational data supported by actual measurements, and the urban internal river channels are uniform, which ensures high completeness and accuracy in the simulation process. Therefore, this coupling model is not suitable for areas with insufficient data or complex inland water system river shapes.

The results of our study can provide reference ideas for subsequent urban flood simulations after sponge city planning and suggest that in the transformation of sponge cities, main pipelines under major roads and overpasses with heavy traffic should be renovated first. This would reduce the extent of the disaster, casualties, and property loss, providing foundational support for subsequent planning processes.

**Acknowledgements** The authors acknowledge the assistance of anonymous reviews.

**Funding** The research was supported by National Key Research and Development (No. 2021YFC3000202), China Power Construction Corporation Technology Project (DJ-HXGG-2021-04), Key R&D Plan Project in Yunnan Province (202203AA080010), Grand Canal Smart River Patrol Application Scenario Construction Project (Phase I) (WR120203A0662023), Monitoring of Integrated Effects of Flood Resource Utilization of Yellow River in the northern margin of Kubuqi Desert (ESKJ2023-001), Tibet Agricultural and Animal Husbandry University graduate innovation program (YJS2024-49).

**Data Availability** Not applicable.

## Declarations

**Ethics Approval** All authors kept the ‘Ethical Responsibilities of Authors’.

**Consent to Participate** All authors gave explicit consent to participate in this work.

**Consent to Publish** All authors gave explicit consent to publish this manuscript.

**Conflict of Interest** The authors declare that they have no conflict of interest.

## References

- Ahmad SS, Simonovic SP (2013) Spatial and temporal analysis of urban flood risk assessment. *Urban Water J* 10(1):26–49. <https://doi.org/10.1080/1573062x.2012.690437>
- Chen X, Ji P, Wu YH, Zhao YJ, Zeng L (2017) Coupling simulation of overland flooding and underground network drainage in a coastal nuclear power plant. *Nucl Eng Des* 325:129–134. <https://doi.org/10.1016/j.nucengdes.2017.09.028>
- Chen J, Tian YY, Zhang SJ, Li YW, Guo ZK (2023) Study of urban flooding response under superstandard conditions. *Water* 15(8):16. <https://doi.org/10.3390/w15081492>
- Chikhi F, Li CC, Ji QF, Zhou XL (2024) Advancing sponge City implementation in China: the quest for a strategy model. *Water Resour Manag* 27. <https://doi.org/10.1007/s11269-024-03784-1>
- Gironas J, Roesner LA, Rossman LA, Davis J (2010) A new applications manual for the storm water management model (SWMM). *Environ Model Softw* 25(6):813–814
- Godara N, Bruland O, Alfredsen K (2023) Modelling flash floods driven by rain-on-snow events using rain-on-grid technique in the hydrodynamic model TELEMAC-2D. *Water* 15(22):14. <https://doi.org/10.3390/w15223945>
- Guoyi L, Jiahong L (2022) Flood risk assessment of Shenzhen City based on TELEMAC-2D model. *Water Resour Prot* 38(05):58–64. <https://doi.org/10.3880/j.issn.10046933.2022.01.015>

- Hashemi M, Mahjouri N (2022) Global sensitivity analysis-based design of low impact development practices for urban runoff management under uncertainty. *Water Resour Manag* 36(9):2953–2972. <https://doi.org/10.1007/s11269-022-03140-1>
- Hu CH, Wu Q, Li H, Jian SQ, Li N, Lou ZZ (2018) Deep learning with a long short-term memory networks approach for rainfall-runoff simulation. *Water* 10(11):16. <https://doi.org/10.3390/w10111543>
- Indrawati D, Yakti B, Purwanti A, Hadinagoro R (2018) Computing urban flooding of meandering river using 2D numerical model (case study: Kebon Jati-Kalibata segment, Ciliwung river basin), 2nd Conference for Civil Engineering Research Networks (ConCERN). E D P Sciences, Inst Teknologi Bandung, Fac Civil & Environm Engn, Bandung. <https://doi.org/10.1051/mateconf/201927004021>
- Kumar P, Debele SE, Sahani J, Rawat N, Marti-Cardona B, Alfieri SM, Basu B, Basu AS, Bowyer P, Charizopoulos N, Gallotti G, Jaakko J, Leo LS, Loupis M, Menenti M, Mickovski SB, Mun SJ, Gonzalez-Ollauri A, Pfeiffer J, Pilla F, Pröll J, Rutzinger M, Santo MA, Sannigrahi S, Spyrou C, Tuomenvirta H, Zieher T (2021) Nature-based solutions efficiency evaluation against natural hazards: modelling methods, advantages and limitations. *Sci Total Environ* 784:27. <https://doi.org/10.1016/j.scitotenv.2021.147058>
- Li JK, Deng CN, Li Y, Li YJ, Song JX (2017) Comprehensive benefit evaluation system for low-impact development of urban stormwater management measures. *Water Resour Manag* 31(15):4745–4758. <https://doi.org/10.1007/s11269-017-1776-5>
- Li G, Zhao HD, Liu CS, Wang JF, Yang F (2022a) City flood disaster scenario simulation based on 1D–2D coupled rain-flood model. *Water* 14(21):21. <https://doi.org/10.3390/w14213548>
- Li SS, Wang ZL, Wu XS, Zeng ZY, Shen P, Lai CG (2022b) A novel spatial optimization approach for the cost-effectiveness improvement of LID practices based on SWMM-FTC. *J Environ Manage* 307:11. <https://doi.org/10.1016/j.jenvman.2022.114574>
- Liao R, Xu Z, Ye C, Shu X, Yang D (2023) Simulation of rainstorm waterlogging in Dahong Drainage Drainage Area based on SWMM and InfoWorks ICM models. *Water Resour Prot* 39(03):109–117. <https://doi.org/10.3880/j.issn.1004-6933.2023.03.013>
- Liu CS, Li WZ, Zhao CC, Xie TN, Jian SQ, Wu Q, Xu YY, Hu CH (2023) BK-SWMM flood simulation framework is being proposed for urban storm flood modeling based on uncertainty parameter crowdsourcing data from a single functional region. *J Environ Manage* 344:13. <https://doi.org/10.1016/j.jenvman.2023.118482>
- Liu CS, Hu CH, Zhao CC, Sun Y, Xie TN, Wang HL (2024) Research on Urban Storm Flood Simulation by Coupling K-means Machine Learning Algorithm and GIS Spatial Analysis Technology into SWMM Model. *Water Resour Manag* 38(6):2059–2078. <https://doi.org/10.1007/s11269-024-03743-w>
- Malcherek A (2000) Application of TELEMAC-2D in a narrow estuarine tributary. *Hydrol Process* 14(13):2293–2300. [https://doi.org/10.1002/1099-1085\(200009\)14:13%3c2293::Aid-hyp29%3e3.0.Co;2-4](https://doi.org/10.1002/1099-1085(200009)14:13%3c2293::Aid-hyp29%3e3.0.Co;2-4)
- Moulinec C, Denis C, Pham CT, Rougé D, Hervouet JM, Razafindrakoto E, Barber RW, Emerson DR, Gu XJ (2011) TELEMAC: an efficient hydrodynamics suite for massively parallel architectures. *Comput Fluids* 51(1):30–34. <https://doi.org/10.1016/j.compfluid.2011.07.003>
- Nash JE, Sutcliffe JV (1970) River flow forecasting through conceptual models part I — a discussion of principles. *J Hydrol* 10(3):282–290. [https://doi.org/10.1016/0022-1694\(70\)90255-6](https://doi.org/10.1016/0022-1694(70)90255-6)
- Ouyang M, Kotsuki S, Ito Y, Tokunaga T (2022) Employment of hydraulic model and social media data for flood hazard assessment in an urban city. *J Hydrol-Reg Stud* 44:15. <https://doi.org/10.1016/j.ejrh.2022.101261>
- Rui S, Weiwei S, Xin S, Zhiyong Y, Jiahong L (2022) Impact of various flood scenarios on urban emergency responses times based on the TELEMAC-2D model. *J Tsinghua Univ (Sci Technol)* 62(01):60–69
- Su X, Shao WW, Liu JH, Jiang YZ, Wang KB (2021) Dynamic assessment of the impact of flood disaster on economy and population under extreme rainstorm events. *Remote Sens* 13(19):21. <https://doi.org/10.3390/rs13193924>
- Tan YQ, Cheng QM, Lyu FW, Liu F, Liu LH, Su YH, Yuan SC, Xiao WY, Liu Z, Chen Y (2024) Hydrological reduction and control effect evaluation of sponge city construction based on one-way coupling model of SWMM-FVCOM: a case in university campus. *J Environ Manage* 349:13. <https://doi.org/10.1016/j.jenvman.2023.119599>
- Voevodin AF, Nikiforovskaya VS (2011) Parameter identification methods of hydraulic models for the study of current water in open channels. *J Inverse Ill-Posed Probl* 18(8):945–954. <https://doi.org/10.1515/jiip.2011.013>
- Wu XS, Wang ZL, Guo SL, Liao WL, Zeng ZY, Chen XH (2017) Scenario-based projections of future urban inundation within a coupled hydrodynamic model framework: a case study in Dongguan City. *China J Hydrol* 547:428–442. <https://doi.org/10.1016/j.jhydrol.2017.02.020>

- Wu XS, Wang ZL, Guo SL, Lai CG, Chen XH (2018) A simplified approach for flood modeling in urban environments. *Hydrol Res* 49(6):1804–1816. <https://doi.org/10.2166/nh.2018.149>
- Xu T, Xie ZQ, Jiang FS, Yang SQ, Deng ZT, Zhao L, Wen GZ, Du QY (2023) Urban flooding resilience evaluation with coupled rainfall and flooding models: a small area in Kunming City, China as an example. *Water Sci Technol* 87(11):2820–2839. <https://doi.org/10.2166/wst.2023.149>
- Yajun F, Chuanqi Y, Xin J, Jianhua L, Lijuan X, Mingxuan R (2021) Research on water-logging control effect of mountain sponge city based on SWMM-CCHE2D unidirectional coupling model. *Eng J Wuhan Univ* 54(10):898–906+941. <https://doi.org/10.14188/j.1671-8844.2021-10-003>
- Yang WC, Zheng CX, Jiang XL, Wang H, Lian JJ, Hu D, Zheng AR (2023) Study on urban flood simulation based on a novel model of SWTM coupling D8 flow direction and backflow effect. *J Hydrol* 621:14. <https://doi.org/10.1016/j.jhydrol.2023.129608>
- Yao S, Chen NC, Du WY, Wang C, Chen CZ (2021) A cellular automata based rainfall-runoff model for Urban inundation analysis under different land uses. *Water Resour Manag* 35(6):1991–2006. <https://doi.org/10.1007/s11269-021-02826-2>
- Yao YT, Li JK, Jiang YS, Huang GR (2023) Evaluating the response and adaptation of urban stormwater systems to changed rainfall with the CMIP6 projections. *J Environ Manage* 347:10. <https://doi.org/10.1016/j.jenvman.2023.119135>
- Zeng ZY, Wang ZL, Lai CG (2022) Simulation performance evaluation and uncertainty analysis on a coupled inundation model combining SWMM and WCA2D. *Int J Disaster Risk Sci* 13(3):448–464. <https://doi.org/10.1007/s13753-022-00416-3>
- Zhang ML, Xu MH, Wang ZL, Lai CG (2021) Assessment of the vulnerability of road networks to urban waterlogging based on a coupled hydrodynamic model. *J Hydrol* 603:15. <https://doi.org/10.1016/j.jhydrol.2021.127105>
- Zhao CC, Liu CS, Li WZ, Tang YH, Yang F, Xu YY, Quan LY, Hu CH (2023) Simulation of Urban Flood Process Based on a Hybrid LSTM-SWMM Model. *Water Resour Manag* 37(13):5171–5187. <https://doi.org/10.1007/s11269-023-03600-2>
- Zhuang QR, Li MR, Lu ZM (2023) Assessing runoff control of low impact development in Hong Kong's dense community with reliable SWMM setup and calibration. *J Environ Manage* 345:13. <https://doi.org/10.1016/j.jenvman.2023.118599>
- Zongxue X, Chenlei Y (2021) Simulation of urban flooding/waterlogging processes: principle, models and prospects. *J Hydraul Eng* 52(04):381–392. <https://doi.org/10.13243/j.cnki.slxh.20200515>

**Publisher's Note** Springer Nature remains neutral with regard to jurisdictional claims in published maps and institutional affiliations.

Springer Nature or its licensor (e.g. a society or other partner) holds exclusive rights to this article under a publishing agreement with the author(s) or other rightsholder(s); author self-archiving of the accepted manuscript version of this article is solely governed by the terms of such publishing agreement and applicable law.

## Authors and Affiliations

Siwei Cheng<sup>1,2,3</sup> · Mingxiang Yang<sup>3,4</sup>  · Chenglin Li<sup>1,2</sup> · Houlei Xu<sup>5</sup> · Changli Chen<sup>5</sup> · Dewei Shu<sup>5</sup> · Yunzhong Jiang<sup>3,4</sup> · Yunpeng Gui<sup>3,4</sup> · Ningpeng Dong<sup>3,4</sup>

✉ Mingxiang Yang  
yangmx@iwhr.com

Siwei Cheng  
maxvivim@163.com

Chenglin Li  
lcllichenglin@163.com

Houlei Xu  
277582905@qq.com

Changli Chen  
changli.chen@foxmail.com



Dewei Shu  
53725025@qq.com

Yunzhong Jiang  
lark@iwhr.com

Yunpeng Gui  
guiyp@iwhr.com

Ningpeng Dong  
dongnp@iwhr.com

<sup>1</sup> College of Water Conservancy and Civil Engineering, Tibet Agriculture and Animal Husbandry University, Linzhi 860000, China

<sup>2</sup> Research Center of Civil, Hydraulic and Power Engineering of Tibet, Linzhi 860000, China

<sup>3</sup> Department of Water Resources, China Institute of Water Resources and Hydropower Research, Beijing, China

<sup>4</sup> State Key Laboratory of Simulation and Regulation of Water Cycle in River Basin, Beijing, China

<sup>5</sup> PowerChina Kunming Engineering Corporation Limited, Kunming, China